Reuse and valorisation of hemp fibres and rice husk particles for fire resistant fibreboards and particleboards

Daniele Battegazzore[1*], Jenny Alongi[2], Donatella Duraccio[3], Alberto Frache[1]

[1] Dipartimento di Scienza Applicata e Tecnologia, Politecnico di Torino, Alessandria campus, Viale Teresa Michel 5, 15121 Alessandria, Italy

[2] Dipartimento di Chimica, Università degli Studi di Milano, Via C. Golgi 19, 20133 Milano, Italy

[3] Istituto per le Macchine Agricole e Movimento Terra (IMAMOTER)-CNR, Strada delle Cacce 73, 10035 Torino, Italy

* Corresponding author: Tel/Fax: +390131229343/+390131229399; e-mail address: daniele.battegazzore@polito.it

ABSTRACT

The present manuscript deals with the reuse and valorisation of agricultural wastes and by-products (namely, hemp fibres and rice husk particles) to produce fire retardant fibreboards and particleboards for applications in biobuilding. Since fire retardancy is one of the most important challenges, a detailed study on the thermal and flame retardant properties of the above materials assembled using starch as the binder and different ammonium dihydrogen phosphate contents as fire retardant agents, is proposed. The combustion properties have been investigated in developing fire conditions, employing a radiating heat flux of 35 kW/m^2 generated by a cone calorimeter. An optimised formulation able to make both fibreboards and particleboards not ignitable has been found and is predicted to be "A2/B" class in the European fire classification for building products. The resultant materials have proven to undergo pyrolysis and not to burn, favouring the formation of a dense and consistent final residue.

Keywords: hemp fibres; rice husk; cone calorimeter; biobuilding; flame retardancy.

1. Introduction

Bio-based products derived from annually renewable agricultural feedstock represent a portfolio of sustainable, eco-friendly and efficient products that may compete with and replace markets currently dominated by oil-based products. Recently, a wide set of materials has been produced using the agricultural wastes or by-products [1]. Indeed, it has been reported that by 2020 about 10% of the base chemicals will come from renewable plant resources. This trend is expected to rise to 50% by 2050 [2,3].

In the present scenario, some attempts concerning natural fibre-reinforced polymers have been reported for applications in building and automotive [4-9]. However, relevant challenges, including homogenization of material chemico-physical features, namely mechanical and flame-retardant properties as well as durability in relation to the atmospheric agents and UV light, are still unsolved. In particular, very few researches have taken in account that, for being used in building, these materials should be fire retardant [10-14]. Unfortunately, all vegetal compounds and derived polymer composites are generally flammable. The easiest and most effective technique for making fire retardant fibreboards and particleboards consists in the production of ready-to-use products [15]. To this aim, different approaches can be carried out: indeed, it is possible to use flame retardant binders or alternatively to treat fibre or particle surfaces with a flame retardant (FR), sometimes in joint action with inorganic fillers. Among FRs commercially available in the market, those having a char-forming or intumescent character have proven to be the most effective for lignocellulosic substrates [16-18]. Among phosphorus-based FRs, ammonium dihydrogen phosphate (ADP) has already exhibited good performances for lignocellulosic substrates [19-21]. As an example, Suardana et al. reported that the burning rate and the weight loss rate decreased when the percentage of ADP used to treat the coconut and jute fibres increased

[19]. In another research, Dorez et al. [21] studied the flax fibre grafting with phosphorus compounds for improving the fire behaviour. Furthermore, ADP as flame retardant is soluble in water and therefore can be easily used in combination with a water-soluble binder.

Without doubt, wood is the main lignocellulosic raw material used in the particleboard industry. Wood flour [22-24] or wood fibres [23,25] are deeply investigated in the literature and widely employed in industrial applications. On the other hand, annual plant wastes, such as flax and hemp shives, bagasse, cotton stalks, small grain and rice straw, peanut husks, rice husks, grape stalks, and palm stalks are valuable raw materials for the production of lignocellulosic-based boards (both fibre- and particleboards) [7,8,26]. Within these, rice husk presents the highest potential for utilization since rice is one of the most consumed cereals in the world [9,27,28]. As far as natural fibres are concerned, hemp is the one which hold some of the highest specific mechanical properties [29,30]. Hemp is a niche crop delivering fibres, shives and seed. The high added value product in the hemp production chain is the long fibre production, thus all the hurdy, dust and short fibres are considered by-products [31].

For making boards, synthetic binders or adhesives are extensively used; the most common of them are phenol-formaldehyde and urea-formaldehyde resins [32]. Recently, some attempts have been carried out in order to replace such chemicals with new adhesives or binders. By this way, more attention to the environment impact and human or animal safety is given. Polyelectrolytes [33], soybean protein [34] and starch [35] are innovative examples for making particleboards with the use of water as dispersing medium. In the last two cases, completely biodegradable materials are also obtained. In the present work, hemp fibres by-products and rice husk particles have been assembled in fibreboards and particleboards using starch as the binder and different ADP contents as the flame retardant agent [36]. The combustion properties of the resultant materials have been investigated by a cone calorimeter under a 35 kW/m^2 heat flux, mimicking the conditions of a real scenario in developing fire

conditions. Furthermore, the best performing formulations have been irradiated also under a 50 kW/m^2 and classified following the European fire classification for building products EN 13823 [37].

To the best of the authors' knowledge, the use of such technique has been rarely attempted [14,38] on the materials under study.

2 Materials

Hemp fibres having a 960 kg/m^3 density [39] (hereafter coded as H) and rice husk with 975 kg/m^3 density [39] (coded as R) were kindly supplied by Assocanapa s.r.l. and S.P. S.p.A., respectively. Corn starch containing 25-28% of amylose content and having a 1500 kg/m^3 density (CERESTAR® RG 03408) used as the binder (coded as S) was purchased from Cargill Inc. ADP, a water soluble ammonium phosphate salt (reagent grade; 1600 kg/m^3 density), was purchased from Sigma Aldrich. All materials were used as received.

3 Board preparation

In order to prepare the fire resistant boards based on hemp fibres and rice husk particles, three formulations were investigated containing starch and ADP. The binder content was maintained constant for both fibreboards and particleboards and used in water solution (4.0 and 6.0 g of starch and water, respectively). Hemp fibre and rice husk particle amounts (5.5 and 4.0 g, respectively) were optimised for the obtainment of mechanically consistent samples as a function of their different density and morphology [39]. In addition, in the base formulation, ADP was added and the effect of its three different amounts investigated (namely, 0.25, 0.5 and 1.0 g, Table 1). These quantities were chosen on the basis of the results already collected by other researchers on cellulose fibres [36].

As far as fibreboard is concerned, its preparation was already described elsewhere [39], *i.e.* 5.5 g hemp fibres were pressed at 150 °C and 10 MPa for 2 min in 50x50x3 mm^3 moulds (*see* Figure 1a). The obtained mat was initially cut for removing the protruding parts (Figure 1b), then impregnated with the starch solution alone or with ADP (Figure 1c) and pressed at an increasing temperature from 110 to 140 °C for 6 min. During that time, the mould was continuously opened and closed in order to expel water vapour. At the end of this process, the mould was pressed at 10 MPa for 1 min and then cooled down to room temperature (Figure 1d). The formulations under investigation are listed in Table 1 where the sample code contains the acronym of the main component (H or R) and ADP amount expressed in g. As an example, H-S-ADP0.5 represents a board made of hemp fibres treated with a water starch solution containing 0.5 g ADP.

The apparent density of the prepared boards was calculated as weight to volume ratio. The ADP-treated fibreboard densities increased by increasing ADP content and ranged from 1060 to 1240 Kg/m^3 (Table 1). The densities attained allow the fibreboards to be classified as high-density materials, according to the ANSI A208.1 standard [40].

The process for producing the particleboards consists of a single press step, as already described [39]. Grained rice husk (4.0 g) was directly mixed with the water solution of binder (or binder and FR mixture) and then pressed in a 50x50x3 mm^3 mould (Figure 1e) following the same process already described for hemp fibres in order to obtain the final materials (Figure 1f).

The ADP-treated particleboard densities were not deeply affected by ADP content and ranged from 930 to 1009 Kg/m^3 (Table 1). The different density of such materials with respect to those containing fibres was ascribed to the different preparation procedure, as well as different filler aspect ratio and morphology, which are reflected by the different presence of voids in the composite structure.

For an industrial exploitation such as in building, it is mandatory that the proposed materials are able to resist to mechanical deformations and stress. Therefore, the storage modulus (E') at 30 °C and 50% R.H. (relative humidity) of both fibreboards and particleboards were assessed by dynamic-mechanical analysis as already reported in a previous study [39]. The data collected in Table 2 for specimens of 50 x 10 x 3 mm^3 confirm that the above materials possess the mechanical properties suitable for making boards (following CSN EN 312 standard [41]) also in presence of ADP.

4 Characterization techniques

Thermogravimetric analyses (TGA) were carried out both in nitrogen and air, from 50 to 800 °C with a heating rate of 10 °C/min, using a TA Q500 thermo balance (TA Instruments) (experimental error: ±0.5 wt.-%, ±1°C). Samples (approximately 20 mg) were placed in open alumina pans and fluxed with nitrogen or air (gas flow: 60 mL/min). $T_{10\%}$ (temperature at which 10% weight loss occurs), T_{max} (temperature at which maximum weight loss rate is achieved) and mass of the final residues at 800 °C were evaluated.

Cone calorimeter tests (Fire Testing Technology, FTT) were performed according to the ISO 5660 standard [42] on 50 x 50 x 3 mm^3 specimens. Samples were placed in the middle of a 100 x 100 mm^2 holder and exposed to 35 and 50 kW/m^2 heat flux in horizontal configuration in an aluminium tray. For each formulation, the test was repeated three times and standard deviation (σ) was calculated as the experimental error for all measured parameters. Time to Ignition (TTI, s), Total Heat Release (THR, MJ/m^2), and Peak of Heat Release Rate (PHRR, kW/m^2), Total Smoke Release (TSR, m^2/m^2), and final residue (%) were assessed. In order to compare the performance of specimens having different weights, THR and PHRR parameters were normalised with respect to the initial mass (MJ/m^2g and kW/m^2g, respectively).

Prior to combustion tests, all samples were conditioned at 23±1 °C and 50% R.H., in a climate-controlled chamber Binder BFK240 for a minimum of 3 days, up to stable weight was reached.

The surface morphology of cone residues was studied using a LEO-1450VP Scanning Electron Microscope - SEM - (beam voltage: 20 kV); a X-ray probe (INCA Energy Oxford, Cu-Kα X-ray source, k=1.540562 Å) was used to perform elemental analysis (EDX, Energy Dispersive X-ray). The samples were pinned up on conductive adhesive tapes and gold-coated.

5 Fire performances

Many classification systems have been developed throughout the world to evaluate and rank the fire performance of products. The official product classification in Europe, "Euroclass system", is not based on cone calorimeter test results but on Single Burning Item (SBI) test performance [43]. In this system, the fire growth rate index (FIGRA) was selected to be the principal classification parameter [43]. Thus, correlating SBI and cone calorimeter test results is a useful tool for the product development as cone calorimeter is a well-established test method that requires only small samples [44]. For this reason, following the report of Hakkarainen [44], two classification indices proposed by Kokkala, Thomas and Karlsson [45] are used: the ignitability index I_{ig} that is the inverse of time to ignition (t_{ig}) and the rate of heat release index I_Q that is obtained by integrating the rate of heat release (*HRR*) in time (*t*), with a higher weight assigned to the rate of heat release values immediately after ignition than to those occurring later. The equations for the two indices are:

$$I_{ig} = 1/t_{ig} \qquad \text{Eq.(1)}$$

$$I_Q = \int_{t_{ig}}^{t_f} \left[\frac{HRR\,(t)}{(t-t_{ig})^m} \right] dt \qquad \text{Eq.(2)}$$

where t_f is the end time of the test, and the integration starts from the moment of ignition t_{ig}. A larger value of the exponent m corresponds to a higher relative significance of the early phases of the test and a smaller contribution to the I_Q index by the heat release rate in the later stages of the test. With these definitions, higher values of each index correspond to a faster rate of fire growth. The two indices are here calculated with m=0.89 and the t_{ig} as the moment when the HRR reaches 50 kW/m^2 from the cone calorimeter test results measured at 50 kW/m^2, as suggested by Hakkarainen [44].

The calculated I_{ig} and I_Q indices are used to predict the *FIGRA* values following the equation:

$$FIGRA = B * I_{ig}^{p1} * I_Q^{p2} \qquad \text{Eq.(3)}$$

The Eq.(3) has been fitted to a great set of experimental data in order to obtain agreement between the experimental and predicted *FIGRA* values. The best fitting values (R^2=0.88) have been calculated as B=3.3×10^{-4}, $p1$=0.70 and $p2$=1.80 for I_{ig} values in the range of 1–12 min^{-1} and measured *FIGRA* values in the range of 50–900 W/s [44].

6. Results and discussion

6.1 Raw materials

In order to better understand the thermal and combustion behaviour of the present boards, a preliminary study on the parent raw materials has been carried out by microscopy, thermogravimetry and cone calorimetry.

6.1.1 Morphological characterization of hemp fibres and rice husk particles treated with ADP

When the raw materials were treated with ADP, it is possible to observe a layer covering the surface of hemp fibres and geometric particles of the recrystallized FR on rice husk particles. From the elemental analysis made on areas with FR particles (points 2 and 4 in Figure 2) and

apparently free zones (points 1 and 3), it is possible to detect the presence of P element: around 1 wt.-% for the point where apparently no fire retardant particles are visible and around 5-10 wt.-% on such particles. Thus, the presence of phosphorous element is evident also in the areas without FR particles, probably covering and partially migrating inside the natural structures.

6.1.2 Thermal stability by thermogravimetry

The thermal and thermo-oxidative stability of raw materials (hemp fibres, rice husk particles, starch) have been carried out by TGA. Figure 3 shows TG and dTG curves in nitrogen (a) or air (b). H and R degradation occurs similarly: in a single step in nitrogen and in two steps in air, as expected for cellulosic materials [46]. Namely, in inert atmosphere, cellulosics thermally degrade by a single step centred around 300-350°C due to the competition of depolymerisation and dehydration reactions. As a consequence, 50-60% of the pyrolysis products are released as volatile species and only the remaining species are converted to a thermally stable residue (*char*) [16]. In air, the competition of these two processes is more significant and the oxygen presence further complicates the thermal degradation of cellulosic substrates. After the first decomposition step, the *char oxidation* to CO and CO_2 follows.

Apart from an initial weight loss due to water, H and R loose more than 50% of their initial weight in nitrogen in 250 and 375 °C range, leaving a residue thermally stable up to 800°C (*see* Figure 3a and residues in Table 3). Due to the presence of silica, R exhibits a higher final residue with respect to that left by H (35 *vs*. 27 wt.-%) [47]. In air, these residues are further oxidized to CO and CO_2 in 375 and 500°C range, although, both H and R still leave significant residues due to minerals and silica [22], respectively.

As far as S is concerned, its thermal behaviour is very similar to those of the two raw materials [10,22] (Figure 3), with the exception of the final residue left at high temperatures in air (*see* Table 3).

In order to better understand the effect of ADP on H and R, some samples have been prepared without binder just for performing thermal and combustion tests. Indeed, such materials cannot be used in biobuilding without a binder as they do not possess sufficient mechanical properties. When fibres or particles are treated with ADP (Figure 3), cellulose sensitization (as anticipation of degradation) has been observed in both atmospheres, as highlighted by the reduction of $T_{10\%}$ values given in Table 3 (*compare* $T_{10\%}$ values of untreated H with those of H-ADP0.5 and H-ADP1, and untreated R with those of R-ADP0.5 and R-ADP1). Cellulose sensitization promotes the char formation in both nitrogen and air, as the final residues are always higher than those left by untreated materials (*see* TG curves in Figure 3 and residues in Table 3). The formed char is able to protect H and R from their thermal degradation, inhibiting and slowing down the heat, mass and oxygen transfer from the environment to the material, according to the literature [16,19,36]. It is important to notice that only TG and dTG curves of formulations containing 1 g of ADP have been shown in Figure 3, as an example of the observed trend. Pertinent data for all formulations are listed in Table 3.

These plots show that the weight loss rate decreases by using 1g of ADP to treat the fibres and anticipates to lower temperatures. This result may be ascribed to the formation of phosphoric acid that is able to phosphorylate the primary hydroxyl group of cellulose to form a phosphorus ester. These esters catalyse the dehydration of cellulose (anticipation), promoting the char formation and unfavouring the depolymerisation (rate decrease) [19].

6.1.3 Combustion tests by cone calorimetry

Hemp fibres, rice husk particles and the corresponding boards treated with only ADP have been tested under a heat flux of 35 kW/m^2 generated by a cone calorimeter. Recently, a study

by Palumbo, Formosa, & Lacasta [13] investigated the fire performance of these materials employing, in that case, a pyrolysis-combustion-flow calorimetry (PCFC) instrument. Cone calorimeter and PCFC are two completely different instruments from a conceptual point of view and are not able to give the same information, being based on the observation of two different scenarios as discussed elsewhere [48,49]. Indeed, cone calorimeter is able to mimic the conditions in a real fire scenario [50]; conversely, PCFC can only give information about the combustion of pyrolysis products. Since the intent is to prepare fibreboards and particleboards for building, the use of cone calorimetry has been proposed here [50,51]. Das et al. [52] have investigated rice husk and other biomass wastes using cone calorimetry but not with ADP as flame retardant.

Table 4 summarises the collected data in this research. Both raw materials exhibited a similar behaviour: H and R ignite in less than 30 s and immediately spread fire, reaching quite rapidly the PHRR (196 and 176 kW/m^2 for H and R, respectively) and releasing a comparable total amount of heat (13.6 and 12.6 MJ/m^2), data similar to what obtained in the literature [32,52]. The small differences between H and R can be attributed to the presence of inorganic silica that is the main constituent of R residue. During combustion, silica forms an ash layer acting as thermal shield to fire and heat [38]. By this way, the resulting HRR and THR values of R-based composites are lower than those of H.

When H and R are ADP-treated, their combustion drastically changes. Indeed, their TTI increases and PHRR and THR values are significantly reduced. The formulations containing 1 g of ADP were even not ignitable. Indeed, H-ADP1 and R-ADP1 underwent pyrolysis and continued to release gases for all the time of heat exposure, measured by the cone laser and reported in the TSR column in Table 4.

The collected results show that ADP can be considered an effective FR; the materials treated with only ADP left a dense residue in both H and R samples.

Both H and R combustion residue (Figure 4a and c) show the same morphology of the original materials: fibres or particles respectively, which polysaccharide/lignin structure has either partially charred or volatilised. Upon treatment with ADP, the hemp fibre structure was preserved whereas the untreated combusted fibres were extremely fragile, turning into a powder under handling. What remain after H-ADP combustion was mechanically strong and composed of hollow fibres whose walls are made of a charred carbon-phosphorus richer material than the burned untreated H fibres (Figure 4b). R-ADP combustion residue morphology is similar to that observed from R combustion (Figure 4d). A limited adhesion between particles has been found but not self-sustaining material as in the case of H. It is probably due to the different materials morphology in form of particles or fibres/mat which affects the interlocking capability of the particles without a binder.

From the elemental analysis, a lot of elements are present in the hemp residues with the main percentage of C, O, K and Ca elements. The composition is slightly different from the white part mainly present on the surface and the black one in the inner part. From a semi-quantitative point of view, the hemp fibres treated with ADP (Figure 4b) show a higher amount of C and P compared to that not treated, as expected from the components of the FR.

R residue consisting of powder is grey on the surface and black in the inner part (Figure 4c), while that left by R-ADP is a completely black coherent solid (Figure 4d). From SEM observation, the R-ADP particles appear partially interconnected or even covered by a P-rich layer. Also in the case of R-ADP sample, a higher content of C and P elements with respect to neat R were registered.

The consistence of the residue found for the treated materials has already been observed in the literature [19]. This peculiarity has been attributed to the char formed by cellulose contained in fibres and due the esterification of phosphoric acid of primary hydroxyl groups of cellulose. Furthermore, the presence of char obstructs the access of oxygen to unburnt

material by insulating and protecting the sample sub-surfaces and inner layers. In doing so, the oxygen, heat and mass transfer is strongly reduced, giving a not completed degradation resulting in black residues in the inner and lower surfaces and in a higher relative content of C element.

6.2 Fibre- and particleboards

6.2.1 Morphological characterization of boards treated with ADP

The addition of ADP to the formulation with starch as the binder never changes the morphological structure of the composites already studied [39], regardless of the raw material type. The only difference shown in the results of EDX analyses revealing the presence of P element (points 1 and 2 in Figure 5), not present in the composition without ADP.

6.2.2 Thermal stability by thermogravimetry

The thermal and thermo-oxidative stability of the untreated and ADP treated fibreboards and particleboards has been studied (Figure 6). The corresponding data are reported in Table 5. The thermal degradation in nitrogen and air of fibreboards and particleboards proceed similarly to what observed for the neat fibres and particles in terms of mechanism (*compare* Figure 3 and Figure 6). The only difference that deserves to be highlighted is the role of starch in the formulation containing also ADP. Due to its polysaccharide nature, it is subjected to ADP action similarly to what happens for the cellulose within H and R. Indeed, due to the char-forming characteristic [16,36], ADP strongly sensitises both natural reinforcements (H and R) and binder (starch) decomposition, as evidenced by the reduction of $T_{10\%}$ and T_{max} values reported in Table 5. The phosphoric acid released at low temperatures favours the formation of a thermally stable char that further decomposes at higher temperatures. Indeed,

H-S-ADP1 and R-S-ADP1 have shown a higher final residue with respect to untreated materials (34 *vs*. 19 wt.-% and 38 *vs*. 25 wt.-% in nitrogen and 6 *vs*. 2 wt.-% and 12 *vs*. 9 wt.-% in air, for H-S-ADP1 and R-S-ADP1, respectively). The same trend has been observed also for the formulations containing a lower ADP amount. Once again in Figure 6a and b only TG and dTG curves of formulations containing 1 g of ADP as an example of the observed trend.

6.2.3 Combustion tests by cone calorimetry

After assessing board combustion properties by cone calorimetry, it is important to highlight that once the binder was added to the base formulation, sample weight was approximately doubled with respect to those consisting of only pressed fibres or particles. Thus, binder strongly increases the combustible mass. In order to correctly compare the efficiency of the different formulations, it was necessary to normalise THR and PHRR parameters with respect to specimen final mass (Table 6). This approach has been proven to be effective for describing the combustion scenario under investigation [53].

First, the role of the binder has been investigated; TTI of materials with starch is more than double with respect to those of raw materials (*compare* TTI values of H and H-S, and R and R-S). Their normalised PHRR values are significantly reduced by the presence of starch (38 and 14% for H-S and R-S, respectively) while the normalised THR and TSR values are almost constant in all formulations, considering the experimental error. Part of these variations may be due to the higher density of the obtained composite materials which exposed a smaller specific surface to the heat source and part to the different behavior of the starch itself. Unfortunately, the presence of binder hinders the formation of a thermally stable residue, as visible comparing the data in the last column of Table 6 (13 *vs*. 10.5 wt.-% and 26.5 *vs*. 18.5 wt.-% for H, H-S, R and R-S, respectively).

The addition of ADP in different amounts progressively enhances the flame retardant performances of prepared materials, as visible by the HRR curves reported in Figure 7, reaching even not-ignitable formulations (namely, H-S-ADP1 and R-S-ADP1). PHRR and THR reductions reported in Table 6 show that the higher ADP amount, the lower are these values, i.e. the better FR properties.

From an overall consideration and taking into account the experimental error, TSR values are almost equal for all formulations that ignited, while, when ignition does not occur, these parameters increase in a remarkable way due to the release of pyrolysis products (from 4 to 374 m^2/m^2 for H-S, H-S-ADP1, and 15 to 281 m^2/m^2 for R-S and R-S-ADP1). This phenomenon is well known in the literature due to the effect of phosphates or polyphosphates applied to cellulosic materials [36] that increase the carbonaceous products.

The visual aspect of the board residue at the end of tests is of interest. The H-S residue is significantly enlarged (the sample reached the height of 9 mm from 3 mm initial thickness) and shows two different structures: in the upper part, it is light grey with impalpable consistence, while in the lower part it is black with a more compact mat (Figure 8a). The colour difference between the two parts is ascribed to different C content: a higher amount in the black zone (point 2) with respect to that in the light one (point 1).

As far as particleboards are concerned, R-S residue shows a thin brown layer on surface (Figure 8b) due to the decomposition products.

Its expansion (9.5 mm height of final thickness) and consistency are similar to what has been observed in the case of hemp fibres. Its morphology reproduces the shape of the original rice husk particles. EDX confirms a high amount of Si element (points 3 and 4 in Figure 8) typical of rice husk and a higher presence of C element in the lower part of the specimen (point 4 in Figure 8) due to the protecting shield of the upper part.

Furthermore, it is interesting to observe the expansion of residue as a function of ADP content. H-S-ADP0.5 residue was expanded more than that left by H-S-ADP1 (11 *vs*. 7 mm of final thickness), that however does not ignite. In both cases, the structure is black (Figure 9a and b). The only aspect to be underlined in the H-S residue is the presence of bubbles on the fibre surface most extensive in the sample that ignites, as evidenced by SEM. Referring to R-S-based formulations, the expansion changes from 15 to 5 mm in the case of ignited or not ignited samples (Figure 9c and d, respectively). SEM micrographs show an interconnected bubble-rich structure with embedded particles for the material that ignited, Figure 9c and less bubble presence in the material that did not ignite Figure 9d. It is likely that 1 g of ADP (the highest concentration under investigation) releases the right amount of phosphoric acid, able to create a thermally stable residue. This latter is capable of inhibiting heat, oxygen and mass transfer from the atmosphere to fibres or particles, preventing their combustion. Moreover, the increase of the charred material leaves less organic volatile release. Meanwhile, the release of water from starch occurs and dilutes the volatile fuel species derived from H or R. The formulations with 1 g of ADP do not allow the fuel mixture to reach the flammability limit and prevent their ignition.

By observing the combustion behaviour, it is possible to note that the high expansion of H-S-ADP0.5 and R-S-ADP0.5 occurs after TTI. Indeed, only a sudden increase of temperature due to the flame spread may produce the release of a high amount of volatiles which increase the quantity of bubbles and the resulting expansion of samples (Figure 9a and Figure 9c).

The samples H-S-ADP1 and R-S-ADP1 did not ignite, thus the generation of fuel gases and water is slow and consequently the expansion is limited (Figure 9b and Figure 9d).

The comparison with other studies is quite complicated. Indeed, in some cases the materials are similar but another measuring technique or setting parameters were used, on the other hand, in other researches, the fillers are similar but the matrices were not bio-based

[13,32,38,51,52,54]. In this scenario, Boccarusso et al. [54] investigated hemp/epoxy composites manufactured by infusion process with 16.32 wt.-% of APP content and found a 74% reduction of PkHRR (187 kW/m^2) with respect to the neat matrix at 50 kW/m^2. Das et al. [52] added rice husk with biochar to PP to manufacture fire retarded composites and found 52% reduction of PkHRR (502 kW/m^2) with respect to neat PP at 50 kW/m^2. Bilal et al. [38] studied the optimum mixture of rice husk-reinforced polyethylene to have the best fire retardant properties and they found for 50 wt.-% of rice husk at 50 kW/m^2 a PkHRR of 808 kW/m^2.

In this study a reduction of the pkHRR at 50 kW/m^2 with respect to not ADP treated materials of 39% for H-S-ADP1 (161 kW/m^2) and 48% for R-H-ADP1 (181 kW/m^2) was registered. Therefore, lower absolute values of pkHRR than those reported in the literature were found but different matrices and samples dimensions were used. For a better comparison, the data obtained in this research were classified in accordance with an European standard in the following paragraph.

6.2.4 Fire performances

In the present study, fire performances were assessed on untreated boards and boards treated with the highest percentage of ADP. The calculated I_{ig} and I_Q indices and the predicted *FIGRA* values with corresponding classification are summarised in Table 7. I_{ig} and I_Q are average values resulting from two cone calorimeter tests at 50 kW/m^2 for each material.

Both the untreated fibre- and particleboard are classified into the category “C” in the EU classification of construction products for resistance to fire, as reported for solid wood panels with high density [37] and better than similar materials (particle and fibreboard) classified as “D” [44]. From the calculated predictions of the ADP-treated boards, the assigned category is the “A2/B”, the best for this Euroclass system. The EU member states are allowed to select

the particular performance appropriate to national requirements also ignoring some parts of the classification, thus no general rules for specific building application are decreed. However, manufacturers must use the entire classification system when supplying construction parts into EU countries and other research can be compared by using this classification.

7. Conclusions

In the present study, the effectiveness of ADP as FR for two agricultural wastes/by-products (hemp and rice husk) has been tested by using a cone calorimeter. The results have shown that such FR agent is able to protect these materials from a 35 kW/m^2 heat flux (*developing fire scenario conditions*), by creating a carbonaceous layer on their surfaces that inhibits the heat, oxygen and mass transfer. The final properties of fibre- and particleboards have proven to be a function of ADP content. Formulations containing 0.25 or 0.5 g of ADP (3-6 wt.-%) drastically increase the TTI of the boards as well as significantly reduce the combustion parameters (THR and PHRR). The highest ADP content (1 g; 10 wt.-%) provides the most efficient solution, as the samples do not ignite. Furthermore, the rate of heat release and ignitability indices are applied to 50 kW/m^2 heat flux tests to predict the European fire classification based on FIGRA values for building products. A prediction of A2/B class for both fibre- and particleboard was reached, the best for this Euroclass system.

The collected results suggest that reuse and valorisation of wastes or by-products from agriculture are possible and allow to design performing materials suitable for building coming 90 wt.-% from renewable resources.

Acknowledgements

The authors want to thank Mr. Fabio Cuttica for cone calorimetry tests, Ms. Giuseppina Iacono for SEM analyses and Prof. Giovanni Camino for fruitful discussion.

Table 1 Codes and compositions of hemp fibre and rice husk particle-based samples.

Sample code	H or R content* [wt.-%]	S content* [wt.-%]	ADP content [g]	ADP content [wt.-%]	Board density$_{\pm\sigma}$** [kg/m^3]
H	100.0	-	-	-	-
H-ADP0.5	91.7	-	0.5	8.3	-
H-ADP1	84.6	-	1.0	15.4	-
H-S	57.9	43.1	-	-	960$_{\pm50}$
H-S-ADP0.25	56.4	41.0	0.25	2.6	1060$_{\pm50}$
H-S-ADP0.5	55.0	40.0	0.5	5.0	1070$_{\pm50}$
H-S-ADP1	52.4	38.1	1.0	9.5	1240$_{\pm50}$
R	100.0	-	-	-	-
R-ADP0.5	88.9	-	0.5	11.1	-
R-ADP1	80.0	-	1.0	20.0	-
R-S	50.0	50.0	-	-	975$_{\pm50}$
R-S-ADP0.25	48.5	48.5	0.25	3.0	950$_{\pm50}$
R-S-ADP0.5	47.0	47.0	0.5	6.0	930$_{\pm50}$
R-S-ADP1	44.4	44.4	1.0	11.2	1009$_{\pm50}$

* the content in grams for all the formulations is 5.5 g for H, 4.0 g for R and 4.0 g for S.

**Only the boards assembled with the binder can be tested for assessing their density.

Table 2 Storage modulus collected by DMA for the boards at 50% R.H.. Dynamic-mechanical analysis (DMA Q800 TA Instruments) in bending configuration. Specimens of 50 x 10 x 3 mm^3 cut from the compression molded boards. Experimental conditions: isothermal tests at 30ºC, 1 Hz of frequency and 0.05% of oscillation amplitude in strain-controlled mode.

Sample code	E' at 30°C$_{\pm\sigma}$ [MPa]
H-S	$1270_{\pm 127}$
H-S-ADP0.25	$1170_{\pm 117}$
H-S-ADP0.5	$1520_{\pm 152}$
H-S-ADP1	$1615_{\pm 162}$
R-S	$1180_{\pm 118}$
R-S-ADP0.25	$1250_{\pm 125}$
R-S-ADP0.5	$1340_{\pm 134}$
R-S-ADP1	$1295_{\pm 130}$

Table 3 Thermogravimetric data of hemp fibres and rice husk particles untreated and treated with only ADP.

Sample code	$T_{10\%}$ [°C]	T_{max}* [°C]	Residue [%]	$T_{10\%}$ [°C]	T_{max1}* [°C]	T_{max2}* [°C]	Residue [%]
	Nitrogen			Air			
H	267	342	27	264	337	448	5
R	275	338	35	267	307	445	17
S	287	308	15	286	305	506	1
H-ADP0.5	226	265	42	230	243-273	516	14
H-ADP1	227	274	36	233	280	491	8
R-ADP0.5	250	299	44	250	290	523	20
R-ADP1	230	291	44	228	281	522	23

*From derivative curves

Table 4 Cone calorimetry data of H and R untreated and treated with ADP.

Sample code	TTI±σ [s]	THR±σ [MJ/m^2] (*reduction, %)*	PHRR±σ [kW/m^2] (*reduction, %*)	TSR±σ [m^2/m^2]	Residue±σ [%]
H	26±3	13.6±1.4	196±15	5±4	13.0±1.0
R	28±3	12.6±1.1	176±15	25±3	26.5±1.0
H-ADP0.5	124±19	4.1±0.4 (*-70*)	96±20 (*-51*)	8±5	25.5±1.0
R-ADP0.5	47±2	4.4±0.8 (*-65*)	143±1 (*-19*)	39±10	33.0±1.0
H-ADP1	N.A.	N.A.	N.A.	224±68	34.0±1.0
R-ADP1	N.A.	N.A.	N.A.	116±20	39.0±1.0

N.A.: data not available as samples do not ignite.

Table 5 Thermogravimetric data of untreated and ADP-treated fibre- and particleboards.

Sample code	$T_{10\%}$ [°C]	T_{max}* [°C]	Residue [%]	$T_{10\%}$ [°C]	T_{max1}* [°C]	T_{max2}* [°C]	Residue [%]
	Nitrogen			Air			
H-S	261	315	19	260	311	418-449	2
R-S	275	312	25	272	308	448	9
H-S-ADP0.25	253	267-304	33	249	265-295	495	5
H-S-ADP0.5	250	261-299	32	252	264-295	514	4
H-S-ADP1	222	245-272	34	228	249-272	522	6
R-S-ADP0.25	250	259-310	36	248	258-302	501	10
R-S-ADP0.5	241	250-304	38	238	246-294	508	12
R-S-ADP1	229	243-301	38	226	241-288	509	12

*From derivative curves

Table 6 Cone calorimetry data of raw materials, fibreboards and particleboards untreated and treated with ADP.

Sample code	TTI±σ [s]	THR/mass±σ [MJ/m^{2}g] *(reduction, %)*	PHRR/mass±σ [kW/m^{2}g] *(reduction, %)*	TSR±σ [m^2/m^2]	Residue±σ [%]
H	26±3	3.6±0.1	51.6±1.8	5±4	13.0±1.0
R	28±3	3.1±0.3	44.0±3.7	25±3	26.5±1.0
H-S	65±6	3.9±0.3	32.1±2.8 *(-38)*	4±1	10.5±2.0
R-S	67±7	3.7±0.1	37.7±4.9 *(-14)*	15±5	18.5±1.0
H-S-ADP0.25	40±6	3.0±0.3 *(-17)*	23.6±3.4 *(-54)*	8±4	18.0±1.0
H-S-ADP0.5	45±2	2.2±0.1 *(-39)*	19.7±0.8 *(-62)*	9±4	23.0±1.0
H-S-ADP1	N.A.	N.A.	N.A.	374±10	34.0±2.0
R-S-ADP0.25	86±16	2.8±0.3 *(-10)*	27.1±2.2 *(-38)*	6±2	30.0±1.0
R-S-ADP0.5	63±7	1.7±0.1 *(-45)*	15.9±1.3 *(-64)*	2±1	34.0±1.0
R-S-ADP1	N.A.	N.A.	N.A.	281±10	39.0±1.0

N.A.: data not available as samples do not ignite.

Table 7 Time to ignition (t_{ig}), Ignitability (I_{ig}) and rate of heat release (I_Q) indices employed for calculating the predicted FIGRA values and SBI classifications (heat flux of 50 kW/m^2).

Sample code	$t_{ig}\pm\sigma$ [s]	$I_{ig}\pm\sigma$ [min^{-1}]	$I_Q\pm\sigma$ [kW/m^2]	Predicted FIGRA$\pm\sigma$ [W/s]	Predicted Class
H-S	42$\pm$5	1.4$\pm$0.2	1036$\pm$55	143$\pm$4	C
H-S-ADP1	45$\pm$7	1.35$\pm$0.2	628$\pm$34	44$\pm$1	A2/B
R-S	38$\pm$8	1.6$\pm$0.4	934$\pm$162	129$\pm$14	C
R-S-ADP1	80$\pm$14	0.76$\pm$0.1	591$\pm$133	28$\pm$7	A2/B
Ordinary particle board*	33*	1.8*	2046*	628*	D*
Medium density fibreboard*	36*	1.7*	2286*	711*	D*

*data from [44]

Figure 1 Digital pictures of pressed hemp fibres (a), hemp mat (b), hemp mat impregnated with water and starch (c), sample H-S (d), slurry of water, starch and rice husk (e) and sample R-S (f).

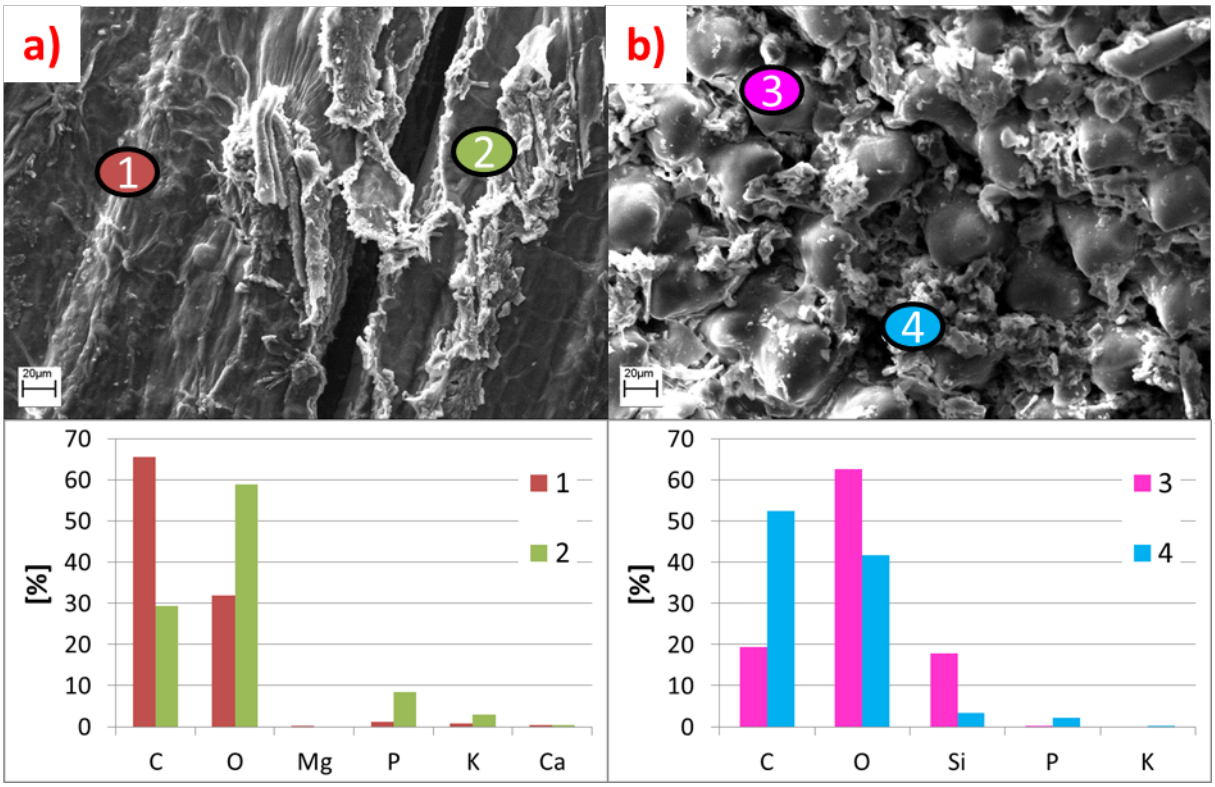

Figure 2 SEM micrographs and elemental analysis of H-ADP1 (a) and R-ADP1 (b).

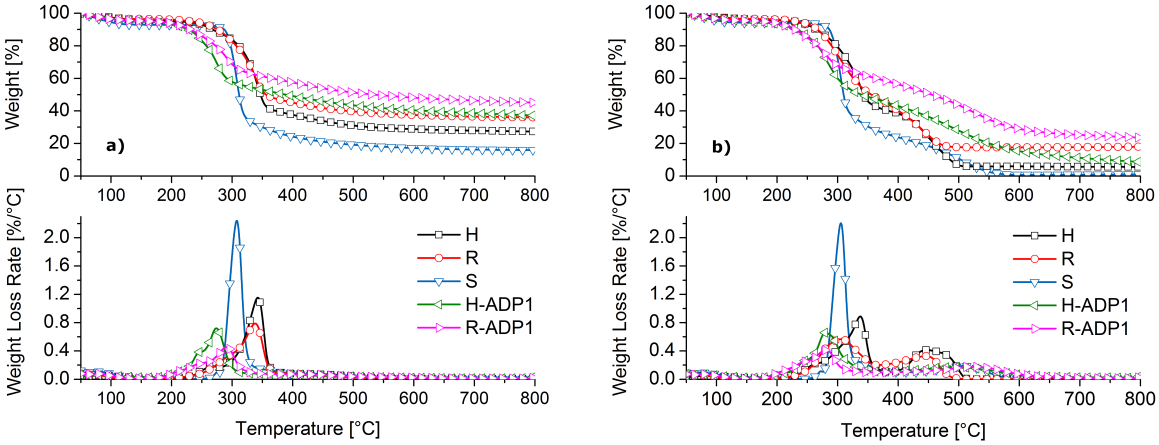

Figure 3 TG and dTG curves of H, R, S, H-ADP1 and R-ADP1 in nitrogen (a) and air (b).

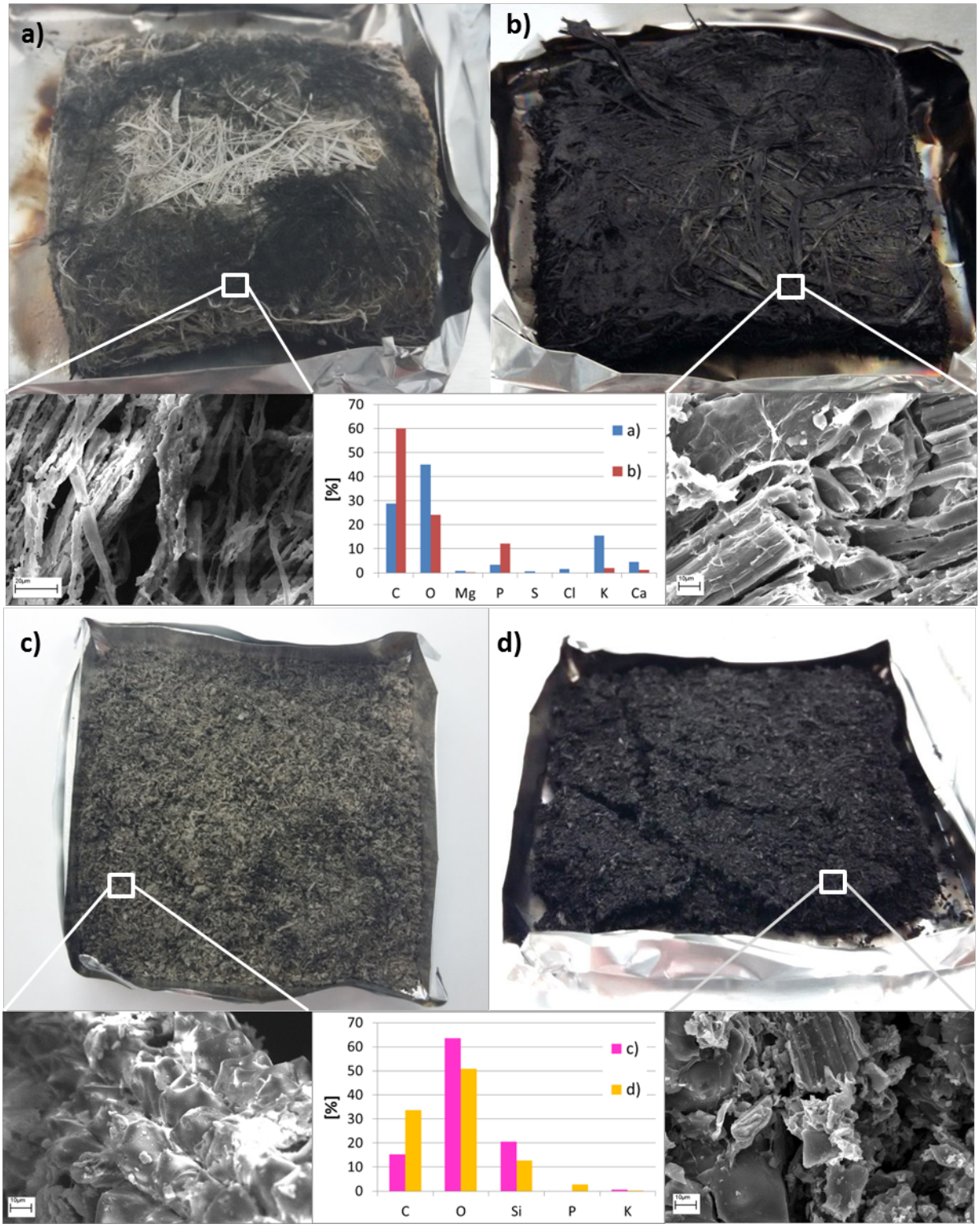

Figure 4 Digital pictures, SEM micrographs and EDX analyses of the final residue for H (a), H-ADP1 (b), R (c) and R-ADP1 (d).

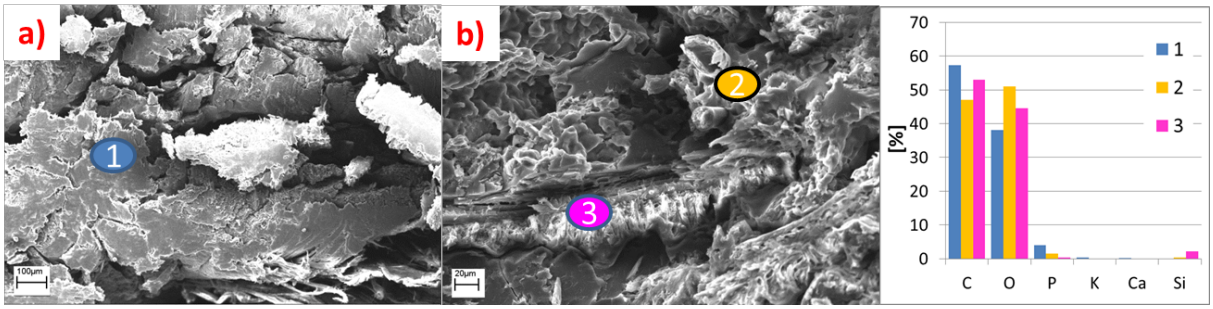

Figure 5 SEM micrographs and EDX analyses of H-S-ADP1 (a) and R-S-ADP1 (b).

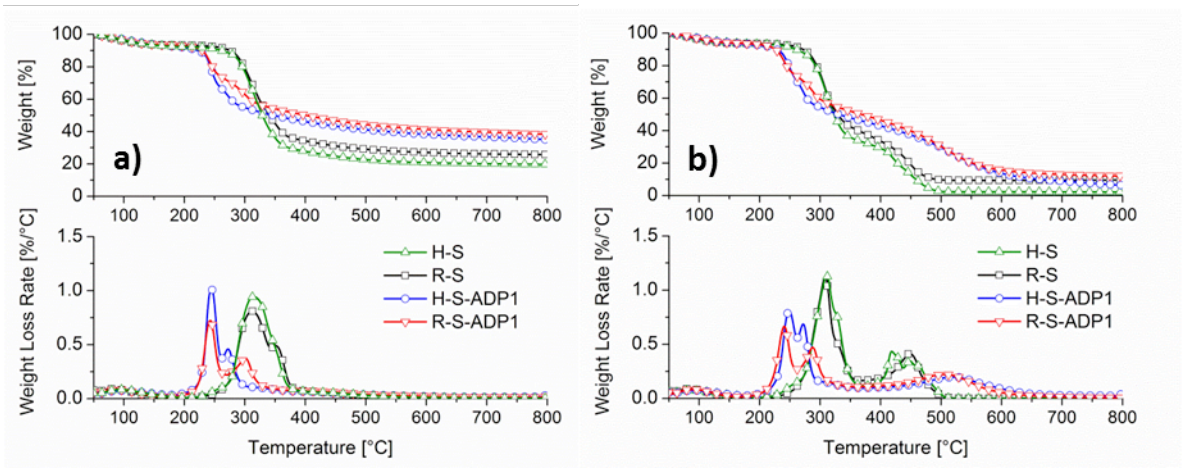

Figure 6 TG and dTG curves of H-S, R-S, H-S-ADP1 and R-S-ADP1 in nitrogen (a) and air (b).

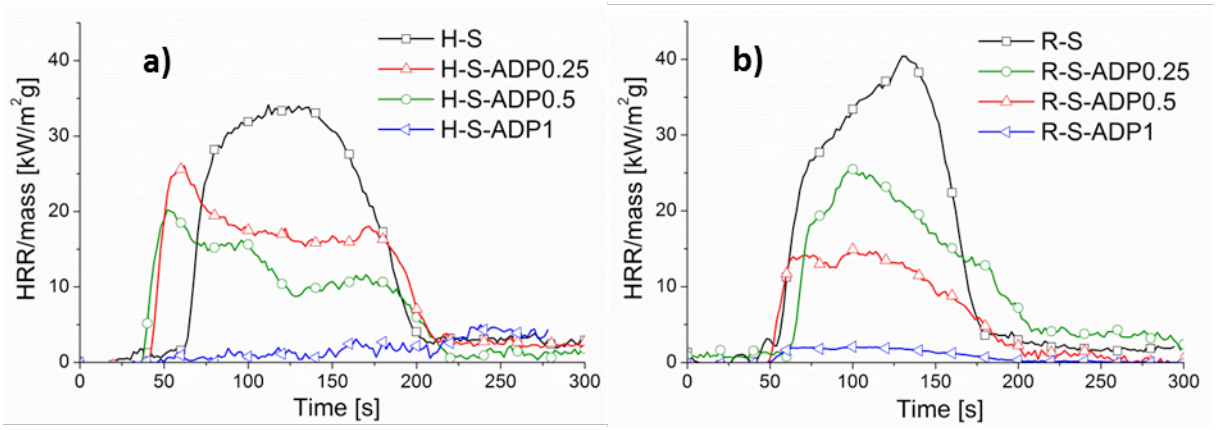

Figure 7 HRR representative curves of untreated H-S (a) and R-S (b), and related ADP-treated materials.

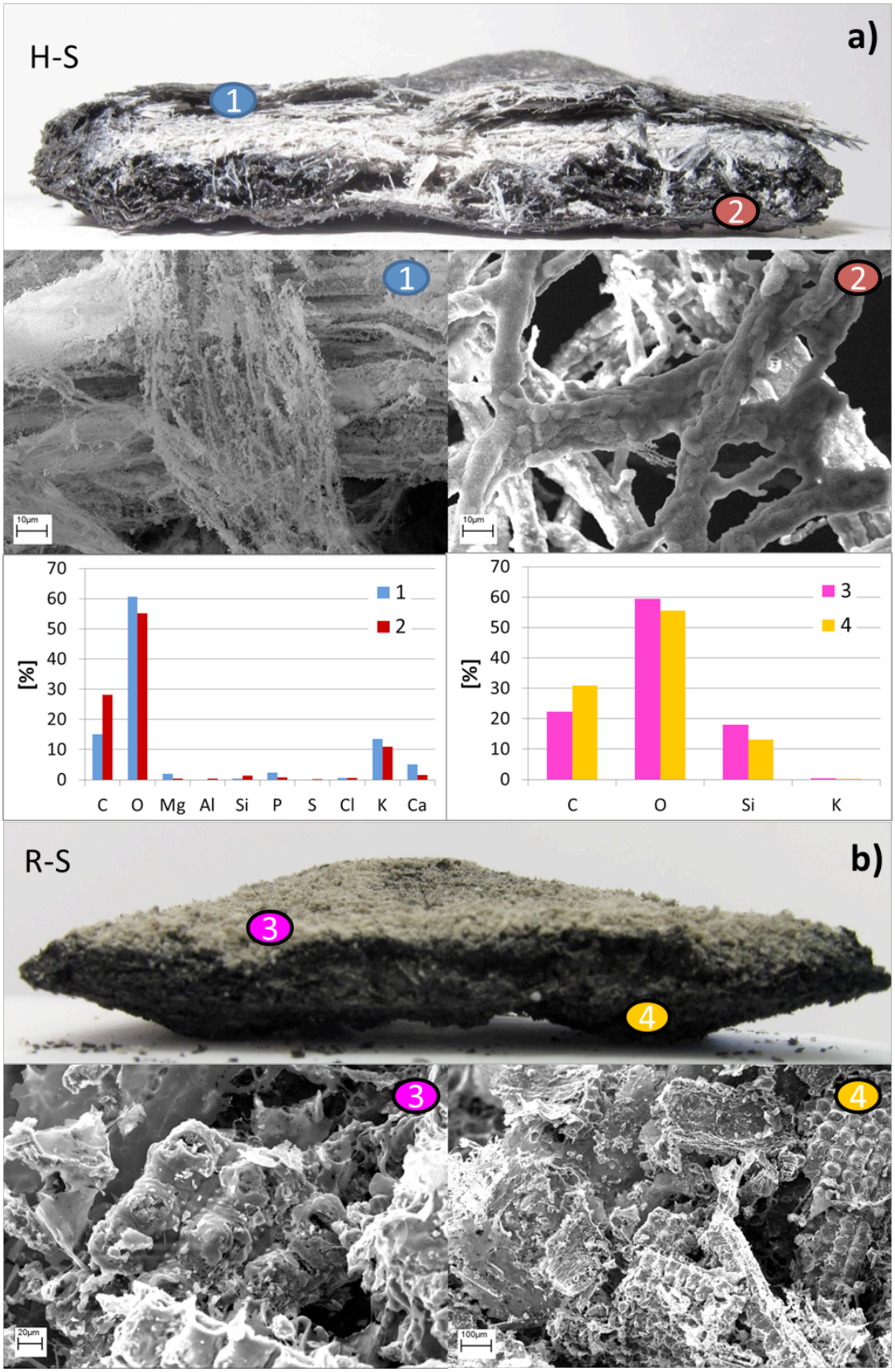

Figure 8 Digital pictures of cone calorimeter residues, SEM micrograph and EDX analyses of H-S (a) and R-S (b).

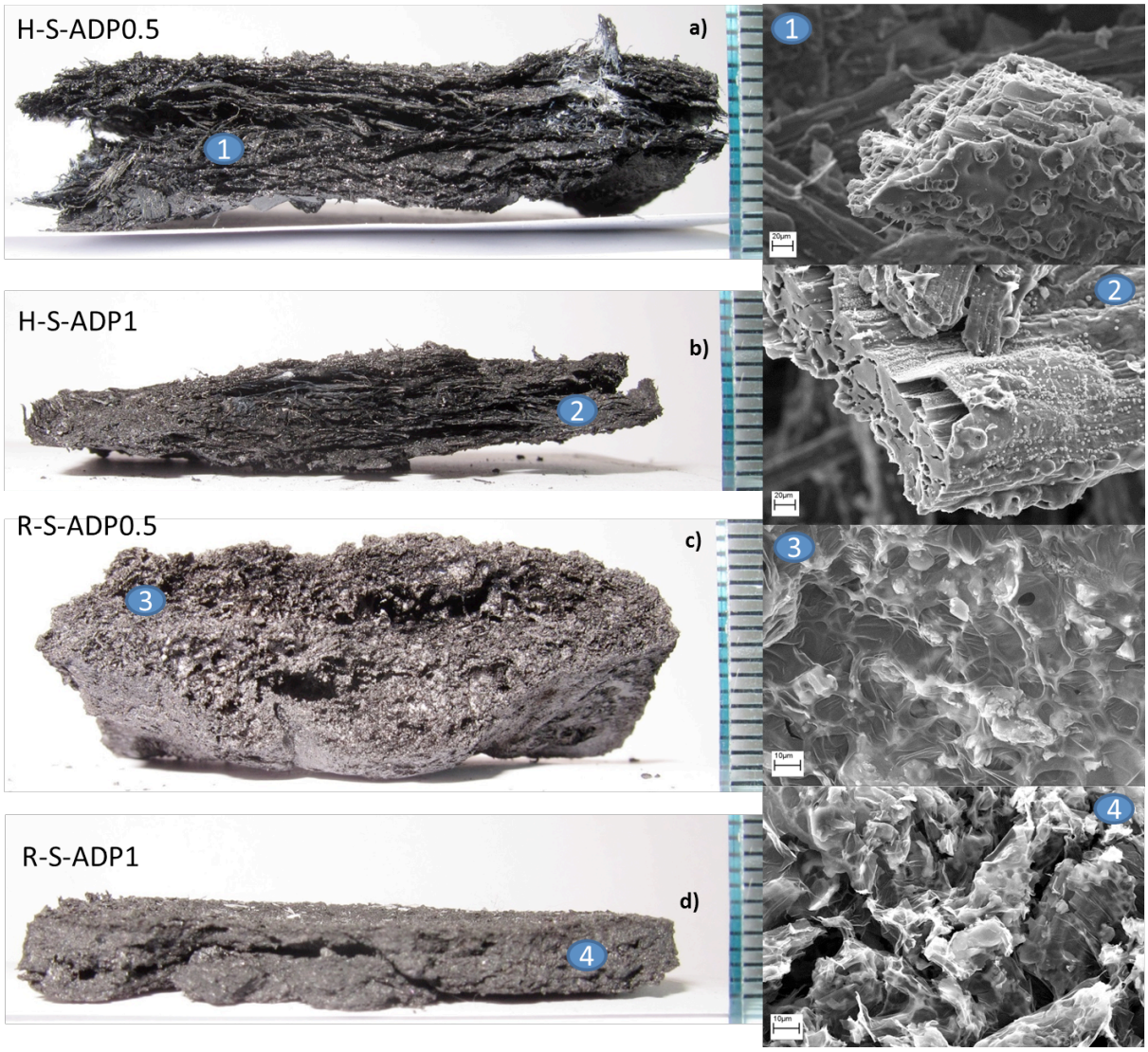

Figure 9 Digital pictures of H-S-ADP0.5 (a), H-S-ADP1 (b), R-S-ADP0.5 (c) and R-S-ADP1 (d) residues.

References

[1] K. Satyanarayana, L. Ramos and F. Wypych, *Biotechnology in energy management*, 2, (2005) 583.

[2] W. Evans, D. Isaac, B. Suddell and A. Crosky, *Natural fibres and their composites: A global perspective*, at: Proceedings of the... Risø International Symposium on Materials Science, 1.

[3] K.G. Satyanarayana, G.G.C. Arizaga and F. Wypych, *Progress in Polymer Science*, 34, (2009) 982.

[4] A.S. Herrmann, J. Nickel and U. Riedel, *Polymer Degradation and Stability*, 59, (1998) 251.

[5] M.J. John and S. Thomas, *Carbohydrate Polymers*, 71, (2008) 343.

[6] G. Koronis, A. Silva and M. Fontul, *Composites Part B: Engineering*, 44, (2013) 120.

[7] R. Kozlowski and B. Mieleniak, *New trends in the utilization of by products of fibre crops residue in pulp and paper industry, building engineering, automotive industry and interior furnishing*, at: Proceedings from the Third International Symposium on Natural Polymers and Composites, Sao Paulo, 504.

[8] M.V. Madurwar, R.V. Ralegaonkar and S.A. Mandavgane, *Construction and Building Materials*, 38, (2013) 872.

[9] N. Padkho, *Procedia Engineering*, 32, (2012) 1113.

[10] V.A. Alvarez and A. Vazquez, *Polymer Degradation and Stability*, 84, (2004) 13.

[11] S. Chapple and R. Anandjiwala, *Journal of Thermoplastic Composite Materials*, 23, (2010) 871.

[12] L. Freivalde, S. Kukle, M. Andzs, E. Buksans and J. Gravitis, *Composites Part B-Engineering*, 67, (2014) 510.

[13] M. Palumbo, J. Formosa and A.M. Lacasta, *Construction and Building Materials*, 79, (2015) 34.

[14] E. Gallo, G. Sanchez-Olivares and B. Schartel, *Polimery*, 58, (2013) 395.

[15] R. Kozlowski, B. Mieleniak, M. Helwig and A. Przepiera, *Polymer Degradation and Stability*, 64, (1999) 523.

[16] J. Alongi and G. Malucelli, *Rsc Advances*, 5, (2015) 24239.

[17] L.A. Lowden and T.R. Hull, *Fire science reviews*, 2, (2013) 1.

[18] Z.N. Azwa, B.F. Yousif, A.C. Manalo and W. Karunasena, *Materials & Design*, 47, (2013) 424.

[19] N.P.G. Suardana, M.S. Ku and J.K. Lim, *Materials & Design*, 32, (2011) 1990.

[20] S.L. Bagga, R.K. Jain, I.S. Gur and H.L. Bhatnagar, *Polymer International*, 22, (1990) 107.

[21] G. Dorez, B. Otazaghine, A. Taguet, L. Ferry and J.M. Lopez-Cuesta, *Polymer International*, 63, (2014) 1665.

[22] D. Battegazzore, J. Alongi and A. Frache, *Journal of Polymers and the Environment*, 22, (2014) 88.

[23] G. Faludi, J. Hári, K. Renner, J. Móczó and B. Pukánszky, *Composites Science and Technology*, 77, (2013) 67.

[24] M. Huda, L. Drzal, M. Misra and A. Mohanty, *Journal of Applied Polymer Science*, 102, (2006) 4856.

[25] K.M. Bogren, E.K. Gamstedt, R.C. Neagu, M. AÅkerholm and M. LindstroÖm, *Journal of Thermoplastic Composite Materials*, 19, (2006) 613.

[26] R. Kozlowski, B. Mieleniak and A. Przepiera, *Zemedelska Technika-UZPI (Czech Republic)*, (1995).
[27] R.R.d. Melo, D.M. Stangerlin, R.R.C. Santana and T.D. Pedrosa, *Materials Research*, 17, (2014) 682.
[28] R.M. Rowell, A.R. Sanadi, D.F. Caulfield and R.E. Jacobson, *Lignocellulosic-plastic composites*, (1997) 23.
[29] K.L. Pickering, M.G.A. Efendy and T.M. Le, *Composites Part A: Applied Science and Manufacturing*, 83, (2016) 98.
[30] S. Kalia, B.S. Kaith and I. Kaur, *Polymer Engineering and Science*, 49, (2009) 1253.
[31] M. Carus, S. Karst, A. Kauffmann, J. Hobson and S. Bertucelli, *European Industrial Hemp Association (EIHA), Hürth (Germany)*, (2013).
[32] R. Kozłowski and M. Władyka-Przybylak, *Polymers for Advanced Technologies*, 19, (2008) 446.
[33] D. Battegazzore, J. Alongi, A. Frache, L. Wagberg and F. Carosio, *Materials Today Communications*, 13, (2017) 92.
[34] E.M. Ciannamea, P.M. Stefani and R.A. Ruseckaite, *Bioresour Technol*, 101, (2010) 818.
[35] A.K. Temitope, *Industrial Engineering & Management*, 04, (2015).
[36] S. Gaan and G. Sun, *Polymer Degradation and Stability*, 92, (2007) 968.
[37] B.A.-L. Östman and E. Mikkola, *Holz als Roh-und Werkstoff*, 64, (2006) 327.
[38] A. Bilal, R.J. Lin and K. Jayaraman, *Journal of Reinforced Plastics and Composites*, 33, (2014) 2021.
[39] D. Battegazzore, J. Alongi, D. Duraccio and A. Frache, *Journal of Polymers and the Environment*, (2017).
[40] in.
[41] in.
[42] in.
[43] in *British Standards Institution, London, UK*, 2002.
[44] T. Hakkarainen, *Journal of fire sciences*, 19, (2001) 284.
[45] M.A. Kokkala, P.H. Thomas and B. Karlsson, *Fire and Materials*, 17, (1993) 209.
[46] J. Alongi and G. Malucelli, *Reactions and Mechanisms in Thermal Analysis of Advanced Materials*, (2015) 301.
[47] D. Battegazzore, S. Bocchini, J. Alongi and A. Frache, *RSC Advances*, 4, (2014) 54703.
[48] B. Schartel, K.H. Pawlowski and R.E. Lyon, *Thermochimica Acta*, 462, (2007) 1.
[49] J. Alongi, F. Cuttica, F. Carosio and S. Bourbigot, *Cellulose*, 22, (2015) 3477.
[50] B. Schartel and T.R. Hull, *Fire and Materials*, 31, (2007) 327.
[51] T.D. Hapuarachchi, G. Ren, M. Fan, P.J. Hogg and T. Peijs, *Applied Composite Materials*, 14, (2007) 251.
[52] O. Das, N.K. Kim, M.S. Hedenqvist, R.J.T. Lin, A.K. Sarmah and D. Bhattacharyya, *Environmental Management*, (2018).
[53] D. Battegazzore, J. Alongi, G. Fontaine, A. Frache, S. Bourbigot and G. Malucelli, *RSC Advances*, 5, (2015) 39424.
[54] L. Boccarusso, L. Carrino, M. Durante, A. Formisano, A. Langella and F. Memola Capece Minutolo, *Composites Part B: Engineering*, 89, (2016) 117.